Sustainable Cities and Society 76 (2022) 103425

Contents lists available at ScienceDirect

Sustainable Cities and Society

journal homepage: www.elsevier.com/locate/scs

Development and transient performance analysis of a decentralized grid-connected smart energy system based on hybrid solar-geothermal resources; Techno-economic evaluation

Yan Cao [a], Hayder A. Dhahad [b,*], Hussein Togun [c], A.S. El-Shafay [d,e], Sagr Alamri [f], Ali A. Rajhi [f], Ali E. Anqi [f], Banar Fareed Ibrahim [g]

[a] School of Mechatronic Engineering, Xi'an Technological University, Xi'an, 710021, China
[b] Mechanical Engineering Department, University of Technology, Baghdad, Iraq
[c] Department of Biomedical Engineering, University of Thi-Qar, 64001 Nassiriya, Iraq
[d] Department of Mechanical Engineering, College of Engineering, Prince Sattam bin Abdulaziz University, Alkharj 11942, Saudi Arabia
[e] Department of Mechanical Power Engineering, Faculty of Engineering, Mansoura University, Egypt
[f] Department of Mechanical Engineering, College of Engineering, King Khalid University, Abha 61421, Saudi Arabia
[g] Department of Information Technology, College of Engineering and Computer Science, Lebanese French University, Kurdistan Region, Iraq

ARTICLE INFO

Keywords:
Distributed generation
Smart energy system
hybrid solar-geothermal energies
thermal energy storage tanks
Thechno-economic

ABSTRACT

The world energy sector is going to change over from its present state of centralized energy generation to a future state with a larger share of distributed generation. In this respect, an innovative smart energy system based on hybrid solar-geothermal energies is proposed in this work, and transient performance assessment and techno-economic analysis are presented to evaluate its dynamic performance applying TRNSYS software. The proposed system is developed to provide power, heating, and cooling demands for a small urban community as the case study. The system consists of PVT panels, thermal energy storage tanks, a turbine, an absorption chiller, and a heat pump as the main components. Also, other subsidiary components like controllers and diverters are incorporated to guarantee the proposed system performance in a smart manner in various ambient conditions of the year. The results show that the system not only provides the annual electrical demand for the considered case study but also a considerable amount of excess power is produced, which can be sold to the power grid to compensate for some expenses of the system. The highest and the lowest exergy efficiency for the proposed system is attained in July and December with the values of 55.9% and 22.8%, respectively. Also, the highest and the lowest values of system unit product cost are obtained for January and July, respectively, as 8.38 and 32.77 $/GJ.

1. Introduction

In developing smart cities to improve the lifestyle, the provision of energy demand is undoubtedly an essential issue (Zhang et al., 2021; Tong et al., 2016). In this regard, Decentralized Energy Systems (DES) based on renewable energy resources offer a promising alternative to a clean environment and sustainable development (Abusaada & Elshater, 2021; Xu et al., 2020). Also, attaining sustainable energy-based development goals requires innovative ideas, among which the Smart Energy Systems (SES) are considered as novel practical concepts (Ahmad et al., 2020; Wang et al., 2021; Xiang et al., 2021). These systems are of further particular interest when they are being powered by renewable energy resources (Harmouch et al., 2018; Xu et al., 2020).

1.1. Decentralized energy systems

Decentralized energy systems are regarded as the systems by which the energy (power, heating, cooling, etc.) is generated near to demand centers Zhu et al. (2020), mainly focused on meeting local energy demands. The World Alliance for Decentralized Energy defines Distributed Generation (DG) as the energy generation near the point of use Singh and Parida (2017). Many advantages for these systems over the centralized energy systems are explained and discussed in the literature, including power quality enhancement and reduction of transmission losses, enhancing the system security and reliability Pesaran et al.

* Corresponding author.
E-mail address: 10592@uotechnology.edu.iq (H.A. Dhahad).

https://doi.org/10.1016/j.scs.2021.103425
Received 13 May 2021; Received in revised form 2 October 2021; Accepted 2 October 2021
Available online 6 October 2021

Nomenclature

A	Area, m^2
c	Product cost, $/GJ
c_P	Specific heat capacity, kJ/(kg.K)
CRF	Capital recovery factor
$\dot{E}$	Exergy rate, kW
G	Total incident solar radiation (W/m^2)
h	Enthalpy (kJ/kg)
h	Convective heat transfer coefficient, W/m^2 K
i_r	Interest rate
$\dot{m}$	Mass flow rate, kg/s
n	Number of system's operating year
N_C	Number of cells in the stack
P	Pressure
$\dot{Q}_a$	Heat absorbed by the panel (kW)
$\dot{Q}_h$	Heat received from the source (kW)
$\dot{Q}_L$	Heat transferred to load (kW)
$\dot{Q}_U$	Useful heat gain (kW)
$\dot{W}$	Power (kW)
T	Temperature (K)
T	The temperature of the sun (K)
U	loss coefficient between the tank and its environment, kJ/(kg.K.m^2)
$\dot{Z}$	Cost rate of components, $/h

Subscripts and abbreviations

Aux	Auxiliary
CCHP	Combined Cooling, heating, and power
Ch	Chiller
DES	Decentralized Energy System
DG	Distribute Generation
DHW	Domestic hot water
F	Fuel
FC	Fuel cell
IC	Internal combustion
HRES	Hybrid Renewable Energy Systems
LCOE	Levelized cost of electricity
P	Product
PEM	Proton exchange membrane
PVT	Photovoltaic/Thermal
SES	Smart Energy System
tot	Total
SES	Smart energy system

Greek letters

τα	transmittance-absorptance product for the PVT panel
η_{PVT}	PVT panels efficiency
η_{ex}	Exergy efficiency

(2020). Also, having low or no carbon emissions for renewable energy-based DG systems is another key advantage (Vera & Jurado, 2018; Duan et al., 2021). With renewable resource utilization, other economic benefits are also attainable such as reduction in fuel consumption and electricity price. A comprehensive survey on motivations, opportunities, and challenges for integration of DES with power systems is presented by Singh and Parida (2017).

Based on the researcher's findings, the DES and DG would play a vital role in the future of electricity networks and systems. These systems have been viewed from different standpoints in literature since their contribution to social and environmental aspects of urban development are diverse Ahmad et al. (2020). Mateo et al. (2019) assessed the influence of natural gas-fueled DG systems on the European electricity distribution networks using techno-economic analysis. They studied six European networks in Italy, Germany, and France and reported great differences in anticipated impact in each considered country. A life cycle assessment based on economic and environmental criteria of DG for building applications is presented by Safaei et al. (2015). They considered three types of cogeneration technologies using solar PV panels. They concluded that, based on the objective of DG employment, a particular operational strategy should be adopted for environmental impacts reduction. Three technologies, including IC engines, fuel cells, and microturbines are compared by Torchio (2015) for CHP systems in DG according to the real demand of a Northern Italian town at real market conditions like fuel and power prices. They indicated a considerable extra electricity generation concerning the users' demand for all the considered CHP options.

Rehman et al. (2019) proposed and optimized a novel PV-based DES for district heating for Nordic conditions. They showed that their proposed system could reduce purchased electricity by 22% in comparison with a centralized solar-based system. The life cycle assessment and conceptual design and of a biomass-fueled PEMFC-based decentralized power generation system is conducted by Suwanmanee et al. (2018). They reported a significant positive impact on global warming compared to the Thai Mixed Electricity Grid. Sun et al. (2019) investigated another grid-connected PEMFC-based decentralized power system under the constant net power mode. They concluded that for transporting more power into the microgrid, the high-load conditions are better, while it yields less flexibility in power changing.

The life cycle assessment for a DG system for CCHP applications driven by solar energy is presented by Yan et al. (2020). They made a comparison between the DG system and conventional centralized energy generation. They used the thermal load following approach and found that their proposed DG system results in a reduction by 46% in global warming impact compared to centralized energy systems.

1.2. Renewable energy-based DG systems

The world energy sector is going to change over from its present state of centralized energy production to a future state with a larger share of DG for its benefits, as explained above. In this regard, utilization of renewable resources to run these systems would result in further environmental and sustainability advantages. Hybrid Renewable Energy Systems (HRES) are inter-connected with more than one energy source and energy conversion units (Bet Sarkis & Zare, 2018). These systems can be powered by various types of power generation technologies, including photovoltaic systems, wind turbines, geothermal energy, fuel cells, micro-turbines, combustion engines, etc. Wind, solar and geothermal energies have been considered as the most preferred renewable energy sources for these purposes (Das et al., 2021; Karami et al., 2014). However, the solar-based HRES is of great interest to which many research works have been devoted Alshammari and Asumadu (2020). Zubi et al. (2020) have indicated significant benefits in terms of economics, sustainability, and emission reductions for a hybrid energy system incorporated with solar collectors, PV panels, and district heating networks in central Europe. In another study conducted in Latvia conditions, it is shown that solar energy could supply 10–78% of total heating energy demand in a district heating system for an urban area with 20,000 inhabitants Soloha et al. (2017). Also, the hybridization of solar energy with other energy resources such as geothermal one is of great importance in the context of HRES Ren et al. (2019).

Recently, these systems are considered promising options to afford power, cooling, heating, and freshwater to the local load connected to local grid networks. In this context, many research works are conducted

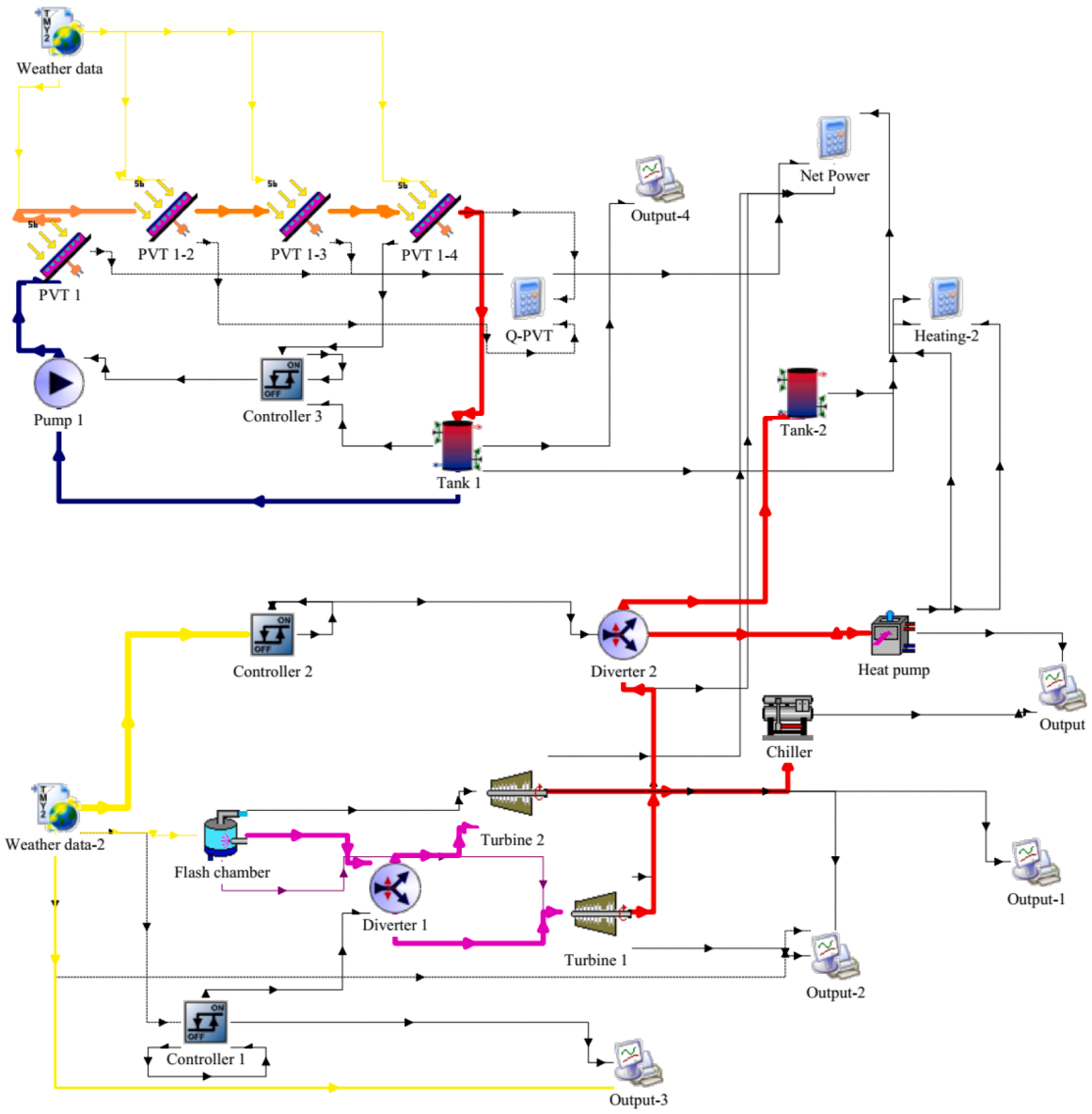

Fig. 1. Flowchart (TRANSYS diagram) of the proposed smart energy system.

mainly focused on CCHP systems since they have been identified as high-efficiency technologies to provide cooling, heating, and power simultaneously Lin et al. (2020). Wang et al. (2019) analyzed a hybrid solar-based CCHP system consisting of solar panels, IC engine, absorption heat pumps, and storage. They reported that the hybrid system integrated with solar energy saves 11.3% of natural gas as compared with the conventional system. Another integrated CCHP system is proposed by Gholamian et al. (2020b) comprised of PVT panels, a micro-GT, and an absorption chiller for an urban building. They conducted a dynamic simulation using TRNSYS software on the system and found that the system has an exergy efficiency of 48.0% with a total product cost of 8.39€/MWh. Nami et al. (2019); Sadi and Arabkoohsar (2019) presented a steady-state simulation of a hybrid solar/municipal waste-fired CCHP system for DG purposes for the energy market of Denmark. They presented thermodynamic and environmental analyzes for their system and reported an exergy efficiency of 28.58%, with a CO2 emission reduction of 445.935 kg-CO2/GJ. For an energy hub in Canada, Ghorab et al. (2019) indicated that the integration of PV panels would result in a reduction of CO2 emissions by 43%, with an approximate 80% cost saving. Li et al. (2019) proposed an innovative solar-powered multi-generation system to provide energy demands for a residential building. They showed that the proposed solar integrated multi-generation system yields 38% higher energy efficiency compared to a single-generation system. Another HRES based on solar energy integrated with a gas turbine is proposed by Yang et al. (2017) for DG purposes. They indicated that the integration of their proposed hybrid system with solar collectors and compressed air energy storage brings about an efficiency increment of 1.02 %. Yang & Zhai (2019) incorporated PV panels and thermal collectors into a conventional CCHP system to build a DG system. They studied the system performance for seven different climate zones and reported the system efficiency as 22.7–29 % for different building types, including hotels, hospitals, and offices. Another solar PV-based CCHP system to provide cooling, heating and electricity demands as a solar-based DG system in southern Italy is investigated by Roselli & Sasso (2016) using dynamic modeling. They found that their proposed system yields primary energy saving by around 40% compared to the conventional fossil fuel-based system. Dynamic techno-economic modeling and optimization of a PVT-based smart energy system for building applications are presented by Behzadi et al. (2020) using TRNSYS software. They showed that their

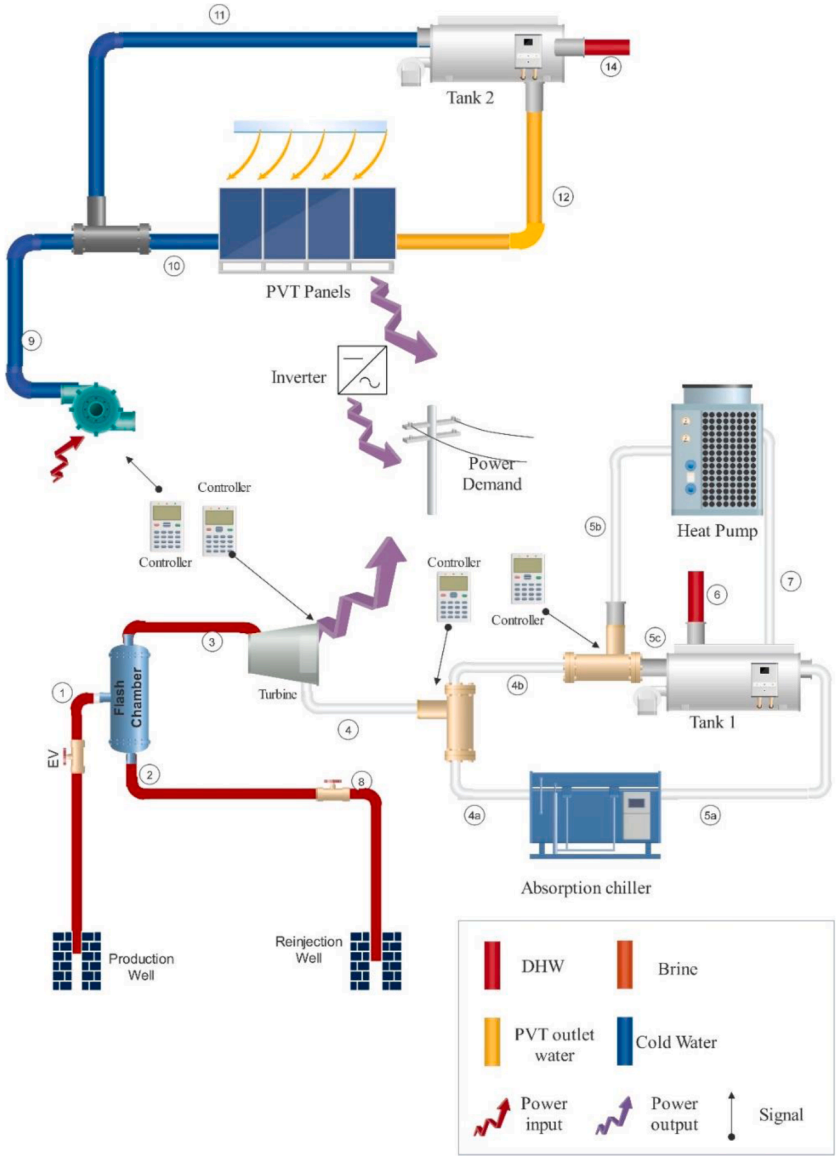

Fig. 2. Schematics of the smart hybrid system.

proposed system could lead to 16.7 €/MWh lower costs for buildings compared to the case if the energy is supplied from the electricity grid. Ferreira et al. (2020) conducted a thermoeconomic analysis for a DG solar energy-powered system with a Stirling engine prime mover and calculated a payback period of around ten years. A comparison between solar thermal collectors and PV arrays in a hybrid CCHP system is made by Wang et al. (2016), who found that the incorporation of thermal collectors more efficiently enhances energy efficiency, while utilization of PV panels improves more efficiently the exergy efficiency. A multi-source DG plant powered by both fossil and renewable resources for CCHP applications is proposed and assessed by Barbieri et al. (2014), who found that the optimal component sizing is significantly related to climatic conditions such as ambient temperature and solar radiation. Khalid et al. (2017) proposed an HRES utilizing hybrid solar and biomass energies for multi-generation purposes (to provide electricity, hot water, cooling, and heating) in a DG system. They calculated exergy efficiency as 34.9% and the LCOE as 0.117 $/kWh.

Some studies have indicated the advantages of the integration of PV panels with heat pumps for DG purposes based on HRES to provide cooling or heating in addition to electricity. Franco and Fantozzi (2016) investigated the feasibility of small-scale integrated PV arrays with a heat pump for a residential building in Pisa, Italy. An HRES system consisting of solar collectors, a district heating network, and a heat pump is proposed and investigated by Kim et al. (2019) to provide the energy demands of a community in Jincheon, South Korea. Their proposed system results in up to 73% of primary energy savings compared to conventional gas-fired boiler systems. Buonomano et al. (2017) studied a CHP plant based on PVT, coupled with office buildings for different weather conditions in Italy. The momentous share of electricity and hot water demand in building is covered by their proposed system. The results indicated a reduction in energy saving and GHG emission respectively around 58.5% and 76.3%. Ibrahim et al. (2014). assessed the thermodynamic investigation of a BIPVT system integrated with a commercial building in Malaysia. The results highlighted that the hourly variation of PVT energy and exergy efficiencies are 55-62% and 12-14%, respectively.

Based on a comprehensive literature survey on HRES for DG purposes, many research works are devoted to solar-powered CCHP systems, and most of these works are focused on small-scale systems for single building applications. Hybridization of solar energy with another qualified renewable resource, namely geothermal one, is rarely noticed in literature for DG purposes.

Table 1
Input data (Compton & Rezaie, 2018; Gholamian et al., 2020b)

Parameter	Value
PVT panel numbers	40
PVT area (m^2)	4
Number of tubes	20
Tube diameter (m)	0.01
Bound thickness	0.01
Bound width	0.01
Emissivity	0.9
Reflectance	0.15
Reference electrical efficiency (%)	20
PV cell reference temperature (°C)	20
Reference thermal efficiency (%)	50
Modifier-temperature (%/°C)	–0.5
Loss coefficient of heat storage tank (kJ/h.m^2.K)	2.5
Thermal efficiency modifier-temperature (%/°C)	– 0.2
Set point temperature for storage tank (°C)	60
Pump efficiency (%)	70
Chilled water temperature (°C)	6.67
Cooling water inlet temperature (°C)	30
Turbine efficiency (%)	90
The total airflow rate of the heat pump (Lit/s)	100
Fresh air Humidity ratio	0.008
Maximum Blower Power for heat pump (kJ/hr)	671.1
Interest rate (%)	20
System economic life (year)	20

1.3. Research motivation and contributions

Recent studies on DG systems have revealed that the incorporation of CCHP systems with hybrid renewable resources can help to enhance local power grid sustainability and reliability. Despite the environmental benefits, the economic and technical aspects of such an integration of DG systems to the power grid should be evaluated, as renewable resources are intermittent naturally and strongly depends on weather conditions Ekanayake (2020). Considering these points, the contributions and objective of this paper can be summarized as:

- Proposal of a novel hybrid solar-geothermal driven DG system to meet electricity, cooling, and heating demands for a small community as a case study.
- Employment of adequate controllers in proper parts of the proposed system to monitor the energy production and consumption rates smartly to switch between appropriate operational modes and proper interaction with the local electricity grid
- Dynamic modeling and transient performance simulation of the system
- Analyzing the overall system and its components considering thermodynamic, technical, and economic performance criteria.

2. System description

The benefits of DG systems and renewable energy resources can be more marked with appropriate integration to provide various energy demands, including electricity, heating, and cooling in various hours of a day and various days/seasons in a year. Fig. 1 illustrates the TRANSYS diagram of the proposed grid-connected CCHP system for a small urban area. As seen, the system consists of two main subsystems: the solar loop and the geothermal loop. In the solar loop via the PVT panels, the solar irradiation is transformed into electricity, and the waste heat of the PV panels is exploited for thermal applications as they are linked to a heat storage tank (Tank 1). The installed Pump 1 sends the water through the PVTs by receiving the control signal from Controller 3 when the ambient temperature is above 26°*C*, while for lower ambient temperatures, Pump 1 is off since the gained thermal energy from the PVT panels is not considerable. As can be seen, the PVT-generated power is a part of the net Power provided by the overall system.

In the geothermal loop, the geothermal brine firstly enters the flash chamber through which the steam is separated from the saturated water. The former goes to Diverter 1 while the latter is reinjected via the reinjection well. For the summer operational mode ($T_{ambient} > 26°C$), the Diverter 1 receives a signal from Controller 1 and sends the exiting steam from the chamber into the Turbine 2 (chiller). The outlet pressure of this turbine is fixed at 100 kPa to provide the steam with a temperature of higher than 90°*C* to drive the absorption chiller to meet the cooling in the summer mode. For operation in heating mode ($T_{ambient} < 26°C$), the exiting steam from the chamber is sent into Turbine 1 by the Diverter 1 via receiving a control signal from Controller 1. The outlet pressure of Turbine 2 is fixed at 60°*C*, with a higher pressure compared to Turbine 1, to attain a higher power amount compared to Turbine 1. The exiting stream from Turbine 1 flows to Diverter 2, which receives ambient temperature signals from Controller 2. For winter mode, when the ambient temperature is below 10°*C*, Diverter 2 sends the stream to the Heat pump to provide the heating effect for district heating demand. However, for the case when: $10°C < T_{ambient} < 26°C$), the Diverter 2 sends the steam into Tank 2 to provide domestic hot water. The modeling and operating strategy in this work is based on the fact that the produced power is firstly utilized to meet real-time demand. If there is no demand at the moment, it is then consumed to heat the water in the storage tank by the electrical coils. When the storage tank is fully charged, and there is no electricity demand, the extra power is transferred to the electricity grid. The operational process of the proposed system is demonstrated more clearly by its schematic diagram in Fig. 2.

The main assumptions to model and analyze the system are as follows (Gholamian et al., 2020b; Wang et al., 2018; Zhang et al., 2016):

1 The pressure losses in the pipelines and the heat losses from the system are neglected.
2 Changes in kinetic and potential energies are neglected.
3 The weather conditions for a Chinese location are considered as the case study in this work.
4 To absorb the rejected heat of condensation and absorption processes in the absorption chiller, a separate cooling tower is not considered.

The given values in Table 1 are assumed for input data and parameters for the system components.

2.1. The weather data and case study

Applying the real site data for solar and ambient conditions is a key factor to achieve the analytical and practical results for the proposed system. The weather conditions of a Chinese location are considered in this work. The hourly ambient temperature throughout the year and its duration curve are shown in Fig. 3. Also, the solar radiation and its duration curve are illustrated in Fig. 4. Fig. 3(a) indicates that the coldest and the hottest days of the year have temperatures of around –15.0°C and 37.4°C, respectively, indicating the necessity of providing both the cooling and heating energies. Fig. 3(b) shows the necessity for providing heating energy for more than 40% of the year, for which the temperature is below 10°*C*. Also, Fig. 4(b) indicates that there exists the potential of solar energy for about 50% of the year, while for around 30% of the year, the intensity of solar radiation exceeds around 200 W.h/m^2. These data are taken from type 109 of TRNSYS software for a typical meteorological year (TMY2) (Compton & Rezaie, 2018; Gholamian et al., 2020b).

As the case study, an urban area containing apartment complexes with 100 units, each of which has the power and hot water demands given in Fig. 5 and Table 2, is considered in this work.

3. System modeling and analysis

The performance of the proposed system is analyzed from exergy, energy, and economic viewpoints. In order to conduct a dynamic

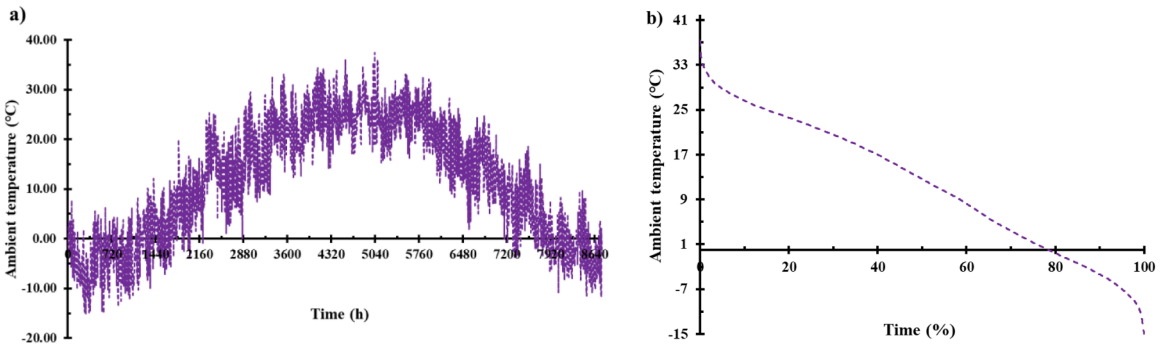

Fig. 3. Yearly variation of real ambient temperature for the considered location.

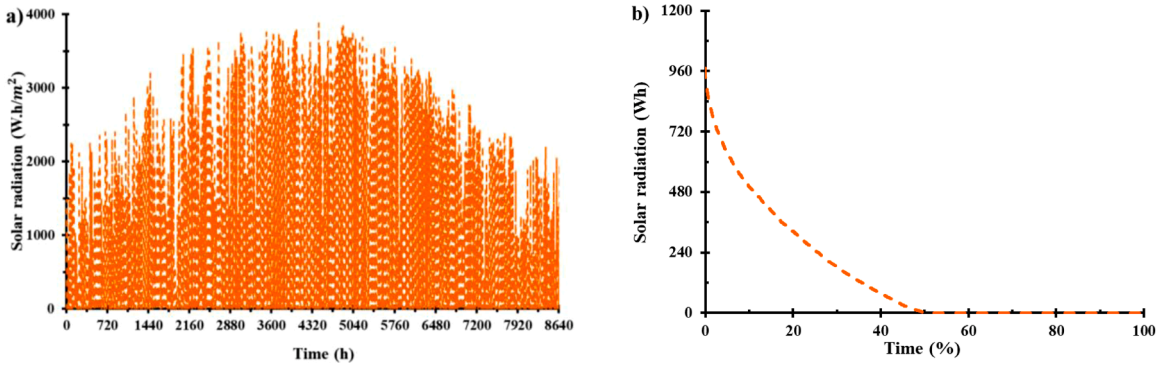

Fig. 4. Annual variation of the solar irradiation for the considered location.

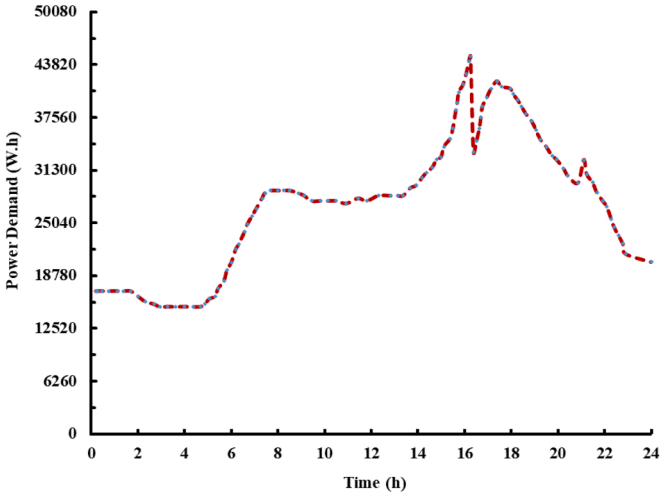

Fig. 5. Load profile of power demand for the considered case study.

simulation on the system performance, the TRNSYS software is used as a transient modeling program with a modular structure. This software solves thermodynamic equations in a transient form based on the considered local weather conditions. Every system in TRNSYS contains several components interacting with each other Song et al. (2017). The components are identified by individual "Type" in this software. For the considered system, the components' types are outlined in Table 3. Details on modeling equations for components in TRNSYS are available in TRNSYS mathematical reference (Reference, n.d.).

3.1. Energy modeling

The energy balance equation as the first-law principle, for a control volume that receives heat and generates power, can be written as (https://www.sciencedirect.com/science/article/abs/pii/S0959652620350563, https://www.sciencedirect.com/science/article/abs/pii/S1359431120336577):

$$\frac{dE_{CV}}{dt} = \dot{Q} - \dot{W} + \sum \dot{m}_{in} h_{in} - \sum \dot{m}_{out} h_{out} \quad (1)$$

3.1.1. PVT panels

The energy balance relation can be applied for any point along the collector surface as Gholamian et al. (2020b):

$$\dot{Q}_{absorbed} = \dot{Q}_{loss,top,conv} + \dot{Q}_{loss,top,rad} + \dot{Q}_{loss,\ back} + \dot{Q}_{u} \quad (2)$$

where $\dot{Q}_{loss,top,conv}$, $\dot{Q}_{loss,top,rad}$ and $\dot{Q}_{loss,\ back}$ denote for heat loss from the top and back of the panels. Also, $\dot{Q}_{u}$ is the useful heat being added to the flow stream inside the collector. These parameters can be calculated as (Arabkoohsar et al., 2021; Luo et al., 2018):

Table 2
Hot water demand for the considered case study (Arabkoohsar, 2019)

Time	Volume (Lit/s)	Duration (min)
10:00	218.4	15
10:30	26.25	10
11:15	218.4	2.5
11:25	26.25	5
11:40	73.5	7.5
12:00	73.5	8
22:00	218.4	15
22:30	26.25	10
23:15	218.4	2.5
23:25	26.25	5
23:40	73.5	7.5
24:00	73.5	8

Table 3
Considered component types in TRNSYS for the main components (Gholamian et al., 2020b; Klein, 1988)

Components	Type	Description
Weather data	Type 109	This component is applied to indicate the yearly weather information based on the typical meteorological year (TMY2) format
PVT panels	Type 563	Type 563 model the PVT panel with the highest efficiency that produces electricity, heat, and cooling simultaneously
Pump	Type 3	This component models a constant flow pump based on user-defined maximum mass flow rate ad power consumption
Storage tank	Type 4	Type 4 models the thermal storage tank integrated with an electrical coil for supplying the building's hot water demand
Absorption chiller	Type 107	This component simulates the thermal-driven absorption chiller to generate cooling from hot water steam
Flow diverter	Type 11	Flow diverter valve works based on an external control signal to specify the split ratio of outlets to obtain a particular temperature
Controller	Type 2	Type 2 models the differential controllers chosen as a function of the difference between upper and lower temperatures
Flow mixer	Type 11	This type of valve mix two inlet streams into an outlet stream
Heat pump	Type 505	Type 505 models a single-stage liquid source heat pump working according to the user-defined input electricity and entering water temperature
Turbine	Type 592	This component simulates a steam turbine based on an isentropic efficiency approach to find the outlet stream's properties
Flash Chamber	Type 611	Type 611 separates the liquid and vapor exhausted from the condenser/expansion valve
Thermodynamic Properties	Type 58	Type 58 delivers two unique independent state properties and calculate the remaining properties

Table 4
cost relations (Aali et al., 2017; Gholamian et al., 2020b)

Component	Cost relation
PVT panel	$Z = c_1 A_{PVT}$ $c_1 = 1060.3$ \$/m^2
Heat storage tank	$Z = c_2 V_{Tank}$ $c_2 = 8945.7$ \$/m^3
Pump	$Z_{Pump} = c_3\ \dot{W}_{Pump}^{0.71}$ $c_3 = 3753.5$ \$/kWh$^{0.71}$
Valve (Diverter, tee piece, tempering valve)	$Z = 159.8$ \$/*unit*
Controller	$Z = 314.4$ \$/*unit*
Chiller	$Z = \dot{Q}_{cooling}(4253.7 \times \dot{Q}_{cooling}^{-0.4662})$
Heat pump	$Z = 100 \times 2677 \times \dot{W}_{HP}^{0.68}$
Turbine	$Z = 6000 \times \dot{W}_{Turbine}^{0.7}$
Flash Chamber	$Z = 5.93 \times \exp(3.49 + 0.488 \times Ln(V_{Chamber}) + 0.107 \times Ln(V_{Chamber}))^2$

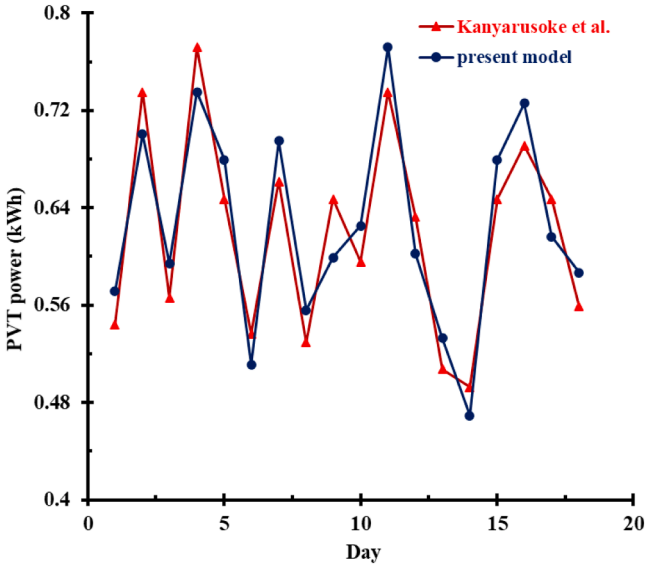

Fig. 6. Verification of the PVT panel's power output (Kanyarusoke et al., 2016)

$$\dot{Q}_{loss,top,conv} = h_{outer} A \left(\overline{T}_{PVT} - T_{amb} \right) \tag{3}$$

$$\dot{Q}_{loss,top,rad} = h_{rad} A \left(\overline{T}_{PVT} - T_{sky} \right) \tag{4}$$

$$\dot{Q}_{loss,\ back} = A \frac{\overline{T}_{abs} - \overline{T}_{inside}}{R_B} \tag{5}$$

$$\dot{Q}_u = \dot{m}_{10} c_P (T_{12} - T_{10}) \tag{6}$$

The absorbed energy expressed by Eq. (2) can also be calculated as Behzadi & Arabkoohsar (2020):

$$\dot{Q}_{absorbed} = GA(\tau\alpha)(1 - \eta_{PV}) \tag{7}$$

In which G and A indicate total incident radiation and panel area. Also, $\tau\alpha$ is the transmittance-absorbance product for the PVT.

The PVT power capacity can be expressed as Gholamian et al. (2020b):

$$\dot{W}_{PVT} = GA(\tau\alpha)\eta_{PV} \tag{8}$$

3.1.2. Absorption chiller

An absorption chiller (single-effect) is used in the considered system to provide cooling. Referring to Fig. 2, the chiller is powered by the exiting hot stream from the turbine. The value of this input energy can be calculated as Gholamian et al. (2020b):

$$\dot{Q}_{Generator} = \dot{m}_{4a}(h_{4a} - h_{5a}) \tag{9}$$

The cooling capacity, which is assumed to be provided by entering 12°C chilled water to the evaporator, can be calculated by:

$$\dot{Q}_{Cooling} = \dot{Q}_{Evaporator} = \dot{m}_{Ch.W}\left(h_{Ch.W,i} - h_{Ch.W,o}\right) \tag{10}$$

where $h_{Ch.W,i}$ and $h_{Ch.W,o}$ denote for the enthalpy of chilled water entering and exiting the evaporator.

3.1.3. Heat pump

In order to provide space heating, a heat pump with an air-cooled condenser is employed in which the inlet fluid (water) temperature to the evaporator is known. As indicated in Fig. 2, for winter operational mode, the exiting stream from the geothermal turbine flows to the heat

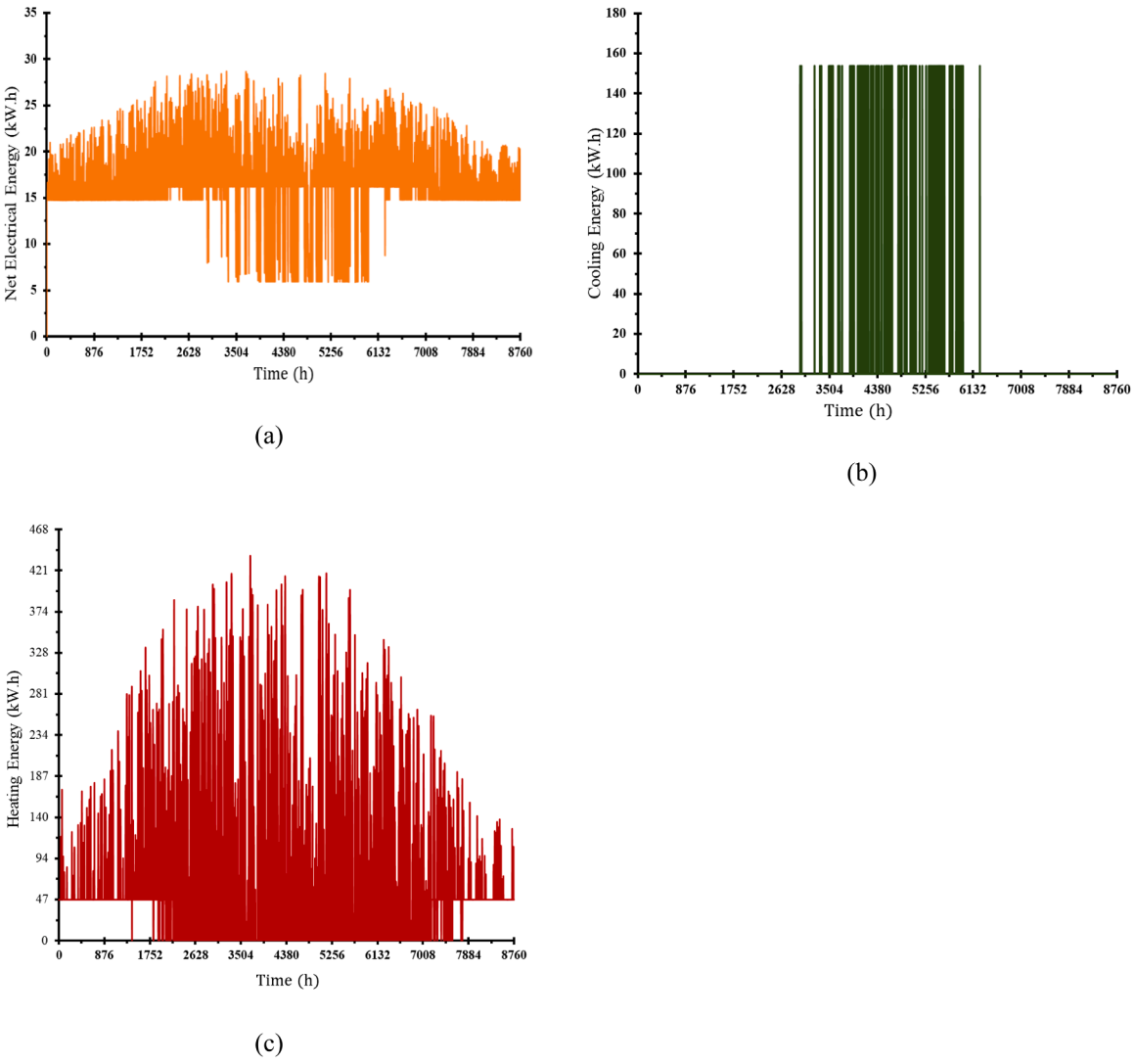

Fig. 7. Annually variation of the generated energy by the system.

pump evaporator to evaporate the refrigerant. The refrigerant rejects heat in the condenser to the airflow, which comes from the ambient at the ambient temperature. Therefore, this heating capacity can be calculated by Gholamian et al. (2020a):

$$\dot{Q}_{Heating} = \dot{Q}_{Condenser} = \dot{m}_{air}\left(h_{air,o} - h_{air,i}\right) \tag{11}$$

The air mass flow rate would be determined by applying the energy balance principle.

3.1.4. Storage tank

In order to provide a steady stream of hot water with the required temperature to the end-user, a tank integrated with an electrical heater using a multi-node strategy is employed. For the *i*th segment of the storage tank, the energy balance in time-basis mode can be expressed as Gholamian et al. (2020b):

$$m_i C_P \frac{dT_i}{dt} = \alpha_i \dot{m}_h C_P (T_h - T_i) + \beta_i \dot{m}_L C_P (T_L - T_i) + UA_i (T_{env} - T_i) + \gamma_i C_P (T_{i-1} - T_i) + \gamma_i C_P (T_i - T_{i+1}) + \dot{Q}_i \tag{12}$$

where α_i, β_i, and γ_i are the various control functions. Also, the $\dot{m}_L$ and $\dot{m}_h$ denote for the mass flow rate of water to the load and from the PVT. T_h and T_L indicate the water temperature entering the tank and the water temperature extracted to supply the load/grid. The U coefficient denotes for the heat loss coefficient from the tank to the surroundings and $\dot{Q}_i$ is the heat input rate by the electrical heater to the *i*th tank node.

The sensible heat rate which is provided by the tank for supplying the load can be explained as:

$$\dot{Q}_L = \dot{m}_L c_P (T_{12} - T_L) \tag{13}$$

Also, the input heat rate to the tank via the hot stream is:

$$\dot{Q}_h = \dot{m}_h c_P (T_h - T_N) \tag{14}$$

Based on these relations, the water towards the load always comes out from the top node, while, the return water from the PVT enters the bottom node (the *N*th node).

3.2. Exergy modeling

The exergy analysis is an essential investigation to evaluate the feasibility of novel thermodynamic systems based on the second law. With negligible variations in velocity and elevation and when no chemical reaction occurs, the only part of the exergy of a fluid stream is the physical one, defined as Gholamian et al. (2020b) (https://www.sciencedirect.com/science/article/abs/pii/S036054422031971X):

$$\dot{E} = \dot{E}_{ph} = \dot{m}[(h - h_0) - T_0(s - s_0)] \tag{15}$$

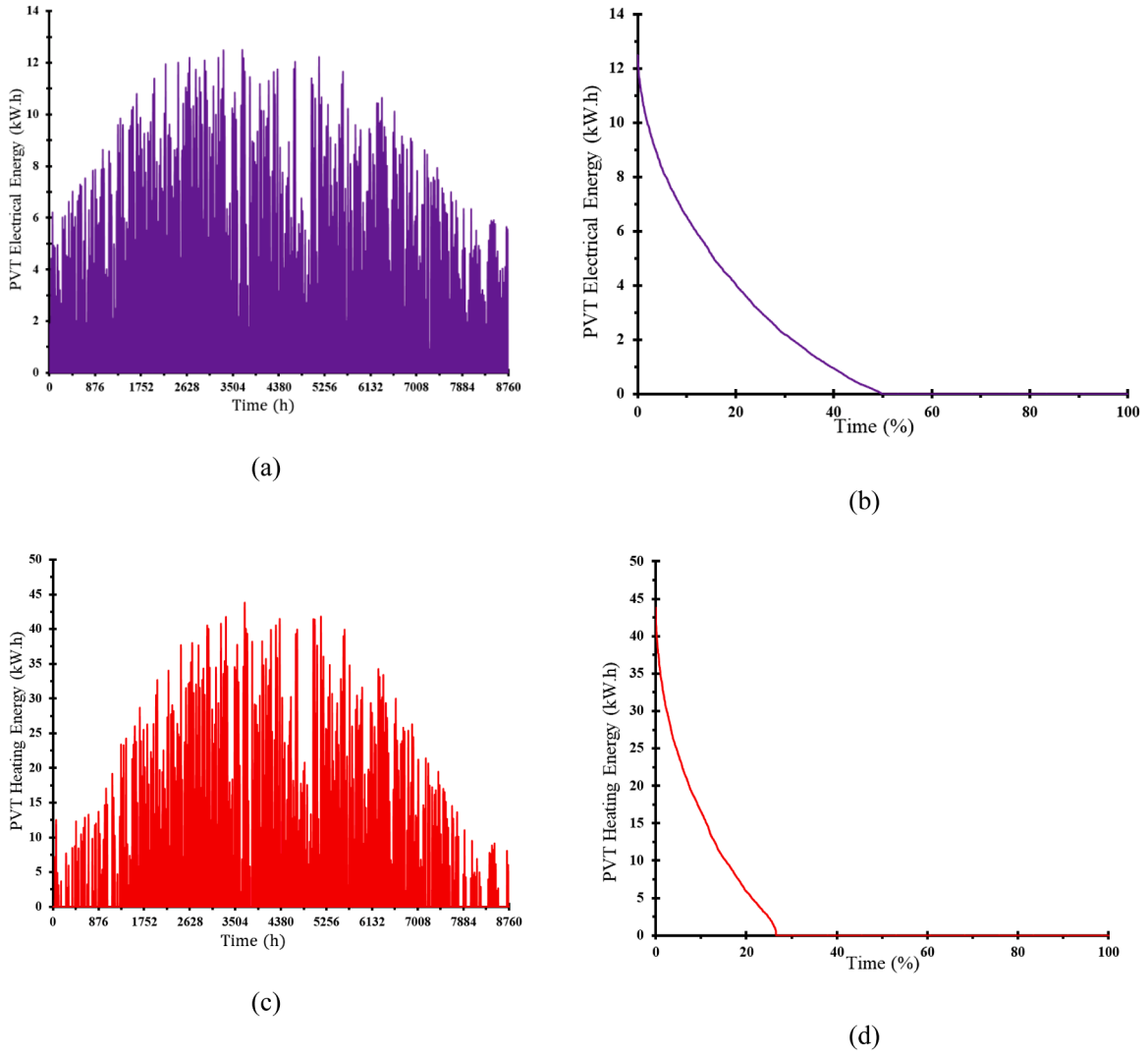

Fig. 8. Annually variation of the generated energy by PVT panels.

The exergy destruction, as an indicator to show the correct inefficiencies in thermal systems' components, is calculated from exergy balance relation as Behzadi et al. (2021) (https://onlinelibrary.wiley.com/doi/abs/10.1002/er.6114):

$$\dot{E}_{D,k} = \sum \dot{E}_{in} - \sum \dot{E}_{out} \tag{16}$$

where, $\dot{E}_{in}$ and $\dot{E}_{out}$ show the entering and exiting exergy flows to the component.

To conduct the exergy analysis on the proposed hybrid system, the exergy input accompanying the solar irradiation is calculated by Habibollahzade et al. (2018):

$$\dot{E}_{solar\ irradiation} = \left[1 + \frac{1}{3}\left(\frac{T_0}{T_s}\right)^4 - \frac{4}{3}\left(\frac{T_0}{T_s}\right)\right]\dot{Q}_{Sun} \tag{17}$$

In which the T_0 and T_s denote for the ambient and equivalent sun temperatures.

3.3. Economic evaluation

Economic considerations and system economic performance can be considered as vital aspects of energy systems. The aim of such an economic evaluation is usually to calculate the system product cost, which can be accomplished by combining conventional economic assessment and exergy analysis. (Bejan, n.d.). To conduct such an evaluation, the investment costs of the system, along with the operational costs, must be assessed. For the *k*th component, the overall cost rate can be expressed as Anvari et al. (2018) (https://www.sciencedirect.com/science/article/pii/S2772427121000127):

$$\dot{Z}_k = \dot{Z}_k^{CI} + \dot{Z}_k^{OM} \tag{18}$$

where, $\dot{Z}_k^{CI}$ and $\dot{Z}_k^{OM}$ denote the investment and OM costs of the component.

The capital recovery factor (*CRF*) can be used to convert the investment cost of a constituent to the annual cost rate Behzadi et al. (2018) (https://www.sciencedirect.com/science/article/abs/pii/S0360319921023338):

$$CRF = \frac{i_r(1+i_r)^n}{(1+i_r)^n - 1} \tag{19}$$

To estimate the investment cost of system constituents the relations given in Table 4 are used.

3.4. Performance assessment

The system performance is assessed from energy, exergy, and economic viewpoints. From the energy perspective, the net output power,

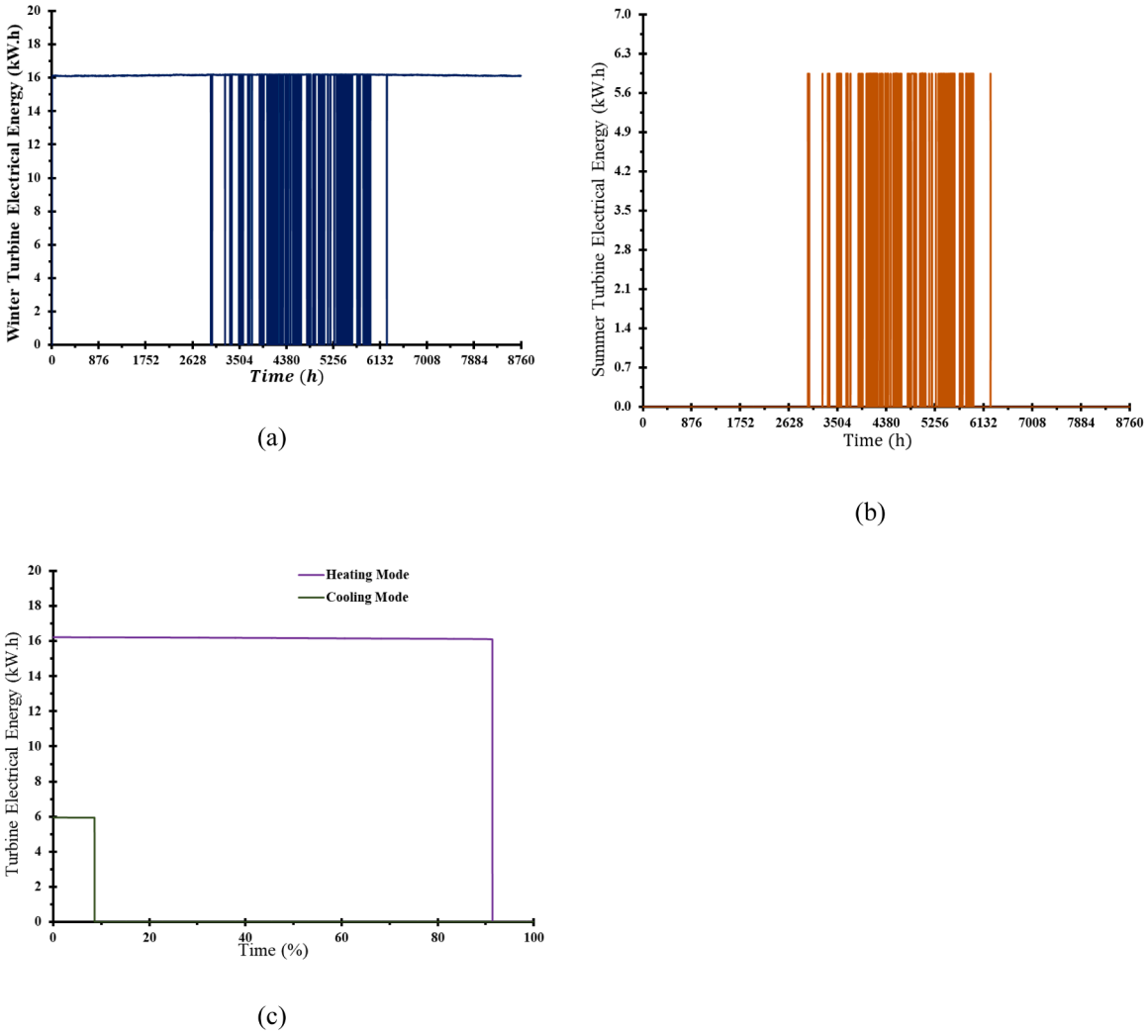

Fig. 9. Annually variation of the generated electrical energy by the turbine.

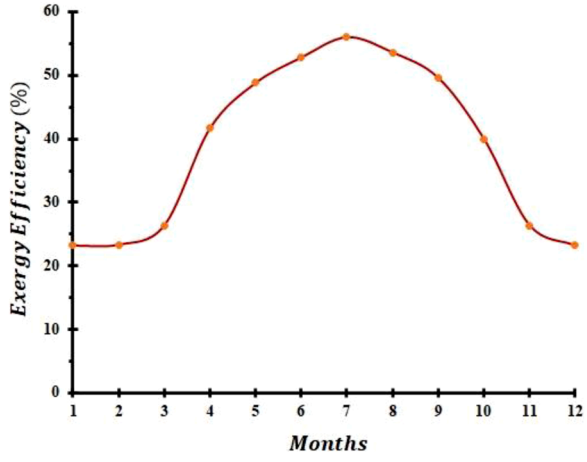

Fig. 10. System efficiency in different months.

output cooling, and output heating are the important performance parameters. The net output power can be calculated as:

$$\dot{W}_{net} = \dot{W}_{net,PV} + \dot{W}_{Turbine} - \dot{W}_{Aux} \tag{20}$$

where, $\dot{W}_{Aux}$ denotes for the consumed power in the system by the pumps (PVT system and chiller) and compressor (heat pump) and the electric heater of the storage tank. Also, by the following relation the value of excess power which can be sold to the power grid can be determined:

$$\dot{W}_{excess} = \dot{W}_{net} - \dot{W}_{demand} \tag{21}$$

The exergetic efficiency is the most important performance indicator from the second law perspective which can be expressed as Gholamian et al. (2020b):

$$\eta_{ex} = \frac{\dot{W}_{net} + \dot{E}_{cooling} + \dot{E}_{heating}}{\dot{E}_{solar\ \ irradiation} + \dot{E}_{geothermal}} \tag{22}$$

where, $\dot{E}_{cooling}$ and $\dot{E}_{heating}$ are the accompanying exergy with the produced cooling and heating. Also, $\dot{E}_{solar\ \ irradiation}$ is the input exergy with solar energy as defined by Eq. (17) and $\dot{E}_{geothermal}$ is the input exergy with geothermal energy.

From the economic standpoint, the unit cost of system products can be taken into account as a key performance indicator. For the considered CCHP system, this parameter is defined as Gholamian et al. (2020b):

$$c_{p,tot} = \frac{\sum_{i=1}^{n_k} \dot{Z}_k + \sum_{i=1}^{n_F} \dot{C}_F}{\sum_{i=1}^{n_p} \dot{E}_p} \tag{23}$$

where $\dot{C}_F$ denotes for the cost rate of entering fuels to the overall system

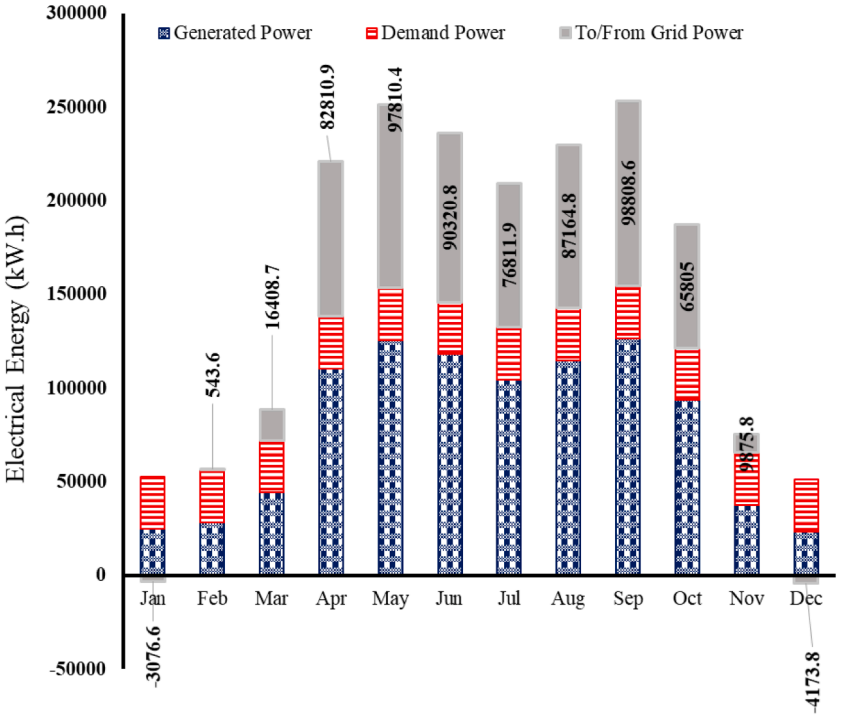

Fig. 11. System generated power in different months.

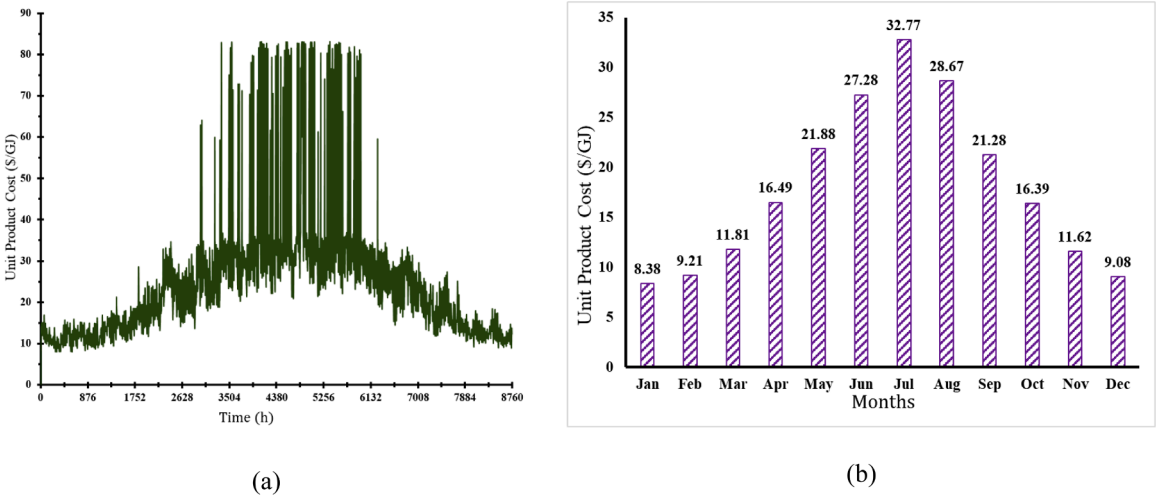

(a) (b)

Fig. 12. Yearly and monthly average unit product cost and of the system.

and $\sum_{i=1}^{n_k} \dot{E}_p$ indicates the exergy rate of system products, including power, cooling, and heating.

4. Results and discussion

To validate the accuracy of developed models, a benchmark of PVT panels modeled in TRNSYS software is used in dynamic form. Fig. 6 shows a good accuracy between the present model and the work carried out by Kanyarusoke et al. (2016) in which the maximum error reaches 5%.

The values of electrical energy, heating, and cooling production by the proposed smart energy system can be considered as the primary performance parameters. The hourly averaged values (along the year) of these parameters are plotted in Fig. 7. Fig. 7(a) indicates that the average generated electrical energy in the summer months is lower compared to winter/fall seasons, despite the higher electrical energy generation by PVT panels in summer for the sake of higher solar radiation. This is due to the lower produced power by the turbine in the summer months as its outlet stream is set to have a higher pressure (and temperature) to run the chiller in hot seasons. The proposed system can generate maximum electrical energy of around 28.7 kW.h, while its minimum value is around 6.1 kW.h in the summer months. Fig. 7(b) indicates that the proposed system can provide 153.9 kW.h cooling energy in the summer months, which is produced by the absorption chiller. Also, from Fig. 7(c) it is found that the average generated heating energy is higher in spring/summer seasons as the solar radiation is higher in these seasons. The chiller exiting stream provides a higher value of heating for domestic hot water (in Tank 1), as represented by Fig. 2. Of course, as shown in Fig. 7(c), in these seasons, lower heating is produced in night hours because no solar radiation exists and the heat pump is not operating.

Table 5
Components cost rates and exergy destruction

Component	$\dot{Z}_k$ for the coldest hour of the year ($/h)	$\dot{Z}_k$ for the hottest hour of the year ($/h)	Exergy destruction (kW.h)
Flash chamber	6.368	6.368	2354.9
Valves	1.1	1.1	510.38
Turbine (in cooling mode)	0	9.5	13179
Turbine (in heating mode)	19.2	0	21965
Pump	0	1.2	94.1
PVTs	36.3	36.3	2670.1
Tanks	25.7	25.7	1817
Chiller	0	44.2	1660
Heat Pump	8.36	0	2540
Controller	2.3	2.3	0
Overall system	99.33	126.67	46790.5
Unit product cost ($/GJ)	7.89	48.1	-

The PVT performance is undoubtedly a crucial factor affecting the overall system performance. Fig. 8 shows the annual variations of heat and power generation by the PVT panels. Also, the duration curves are indicated in this figure. As Fig. 8(a) and 8(c) indicate, the highest values of electrical energy and heat are generated during the summer days when the solar radiation energy is higher. The corresponding maximum values can reach around 12.5 and 43.4 kWh for the power and heat at the $3550-3600th$ hour of the year, respectively. Fig. 8(b) indicates the ability of PVTs to provide electricity for around 50% of the year. However, the efficient heat generation by the panels is limited to around 27% of the year, for which the ambient temperature is high enough. Regarding these results, the standalone PVT system cannot provide total energy demand for the considered case study throughout the year. Therefore the hybrid solar-geothermal energy system is proposed.

Fig. 9 represents the annual variation and duration curve of the generated electrical energy by the turbine, which is powered via geothermal energy. As can be seen, more electrical energy is generated when the system operates in heating mode compared to the operation in cooling mode. This is due to the higher turbine outlet pressure in cooling mode, which is necessary to provide the required higher temperature flow for running the chiller. Therefore in this mode, the turbine generates lower energy. It can be seen from Figs. 9(a) and 9(b) that the turbine maximum electrical energy generation is around 16 and 6 kW.h, respectively, in winter and summer operational modes. Also, Fig. 9(c) indicates that the turbine generates lower power when the overall system operates under the cooling mode for around 10% of the time of the year (for higher ambient temperatures than $26^{\circ}C$) and the rest of the year, the turbine generates higher power values which in this case the overall system operates in heating mode.

The system exergy efficiency is shown in Fig. 10 for all the months of the year. Referring to this figure, lower efficiency values are obtained for cold climates and the winter season. This is rational because by decreasing the ambient temperature, the PVT panels generate lower electrical and heating energies. So, the rate of useful energy transferred from the sun to the working fluid reduces (please see Eq. (22)). The figure indicates the highest efficiency occurs in July with 55.9%, while its lowest value is obtained as 22.8% for December.

Fig. 11 shows the values of generated power for 12 months of the year. Also, the figure represents the demand power and the power to/from the grid. The last parameter indicates the surplus or shortage values for electrical energy, which can be transmitted to/from the grid. Referring to Fig. 11, in two months of the year, namely January and December, the generated electrical power by the proposed system is not enough to provide the demand for the considered community as the case study. This is due to the lower power generation by PVT panels in these months. Therefore, in these months, the shortage values of power as 3076.6 and 4173.8 W.h should be bought from the grid. However, for the rest ten months of the year, the proposed system generates more extra power than that is required for the considered case study. This surplus power can be sold to the grid to compensate for some of the expenses of the considered energy system. The maximum value of extra power is obtained in May and September by more than 97000 kW.h. This is why in these months, the ambient temperature is around the indoor comfort temperature, and the heating/cooling subsystems operate with lower capacity and consumes low power.

To indicate and evaluate the system's economic performance, the unit product cost of the system is calculated and illustrated in Fig. 12. The figure shows higher cost values in the summer season, which can mainly be attributed to the higher cost of cooling production in summer and also the lower value of net power produced in summer. Also, the lower values for unit product cost obtained in winter are mainly due to the higher power production by the turbine, as shown in Fig. 9(a). From Fig. 12(b), the highest and the lowest values of unit product cost is obtained for January and July, respectively, as 8.38 and 32.77 $/GJ.

To have e better view of component-level system performance, the components' cost rate ($\dot{Z}_k$) and exergy destructions are outlined in Table 5. These results are presented for the coldest and hottest hour of the year as the most critical operating cases. Based on the 2nd law of thermodynamics, the main sources of exergy destruction are mixing, the high-temperature difference between the fluids, and chemical reaction. It can be seen that the highest exergy destruction value is obtained for the turbine. The turbine operating in winter mode (heating mode) has a higher exergy destruction value as it works with a higher load in this case. The table further reveals that PVT panels are another source of irreversibility due to the high-temperature difference between the sun and the working fluid. Also, referring to Table 5, the chiller and PVT panels have the most significant values of cost rates among the system components. The higher value for the chiller's cost rate is the main responsible for having a higher overall system cost rate, as a result of which a higher value for unit product cost is attained for the hottest hour of the year.

5. Conclusions and recommendations

In this paper, a novel hybrid renewable energy-based smart energy system is proposed to meet the power, heating, and cooling demands of a small community as the case study. The system consists of solar PVT panels, thermal storage tanks, a turbine, an absorption chiller, and a heat pump. No battery is incorporated into the system to make it cheaper, while the system has a two-way interaction with the local electricity grid. Transient performance analysis is conducted based on technical, thermodynamic, and economic criteria using TRNSYS software. It is concluded that the standalone PVT system cannot provide total energy demand for the considered case study throughout the year. Therefore the hybrid solar-geothermal energy system is proposed. The results also revealed that the system not only provides the annual electrical demand for the considered case study but also a considerable amount of excess power is produced, which can be sold to the power grid to compensate for some expenses of the system. Other essential findings can be summarized as:

- The highest and the lowest exergy efficiency for the proposed system is attained in July and December with the values of 55.9% and 22.8%, respectively.
- In January and December, the generated electrical power by the proposed system is not enough to provide the demand for the considered case study. However, for the rest ten months of the year, the proposed system generates considerable extra power than the case study demand.
- The highest and the lowest values of system unit product cost are obtained for January and July, respectively, as 8.38 and 32.77 $/GJ.

- The highest exergy destruction values are obtained for the turbine and the PVT panels.
- The absorption chiller and PVT panels have the largest values of cost rates among the system components.

Eventually, some recommendations for future extension of the studied research can be suggested as below:

- Analyzing and comparing techno-economic-environmental indicators of the studied system against the same system equipped with other types of chiller or solar collector.
- Studying the feasibility of adding PVTC (Photovoltaic thermal cooling) panels that works based on radiative cooling at night for multi-generation of electricity, heat, and cooling.
- Applying multi-objective optimization to the proposed system to ascertain the most operating condition from various facets simultaneously.

Declaration of Competing Interest

The authors declare that there is no conflict of interest.

Acknowledgment

The authors extend their sincere appreciation to the Deanship of Scientific Research at King Khalid University for the support they received through research groups program under grant number (R.G.P 1-328-42).

References

Aali, A., Pourmahmoud, N., & Zare, V. (2017). Exergoeconomic analysis and multi-objective optimization of a novel combined flash-binary cycle for Sabalan geothermal power plant in Iran. *Energy Conversion and Management, 143*, 377–390. https://doi.org/10.1016/j.enconman.2017.04.025

Abusaada, H., & Elshater, A. (2021). Competitiveness, distinctiveness and singularity in urban design: A systematic review and framework for smart cities. *Sustainable Cities and Society, 68*, Article 102782. https://doi.org/10.1016/j.scs.2021.102782

Ahmad, T., Zhang, H., & Yan, B. (2020). A review on renewable energy and electricity requirement forecasting models for smart grid and buildings. In *Sustainable Cities and Society* (102052,, *55*. Elsevier Ltd. https://doi.org/10.1016/j.scs.2020.102052

Alshammari, N., & Asumadu, J. (2020). Optimum unit sizing of hybrid renewable energy system utilizing harmony search, Jaya and particle swarm optimization algorithms. *Sustainable Cities and Society, 60*, Article 102255. https://doi.org/10.1016/j.scs.2020.102255

Anvari, S., Khalilarya, S., & Zare, V. (2018). Exergoeconomic and environmental analysis of a novel con fi guration of solar-biomass hybrid power generation system. *Energy, 165*, 776–789. https://doi.org/10.1016/j.energy.2018.10.018

Arabkoohsar, A. (2019). Non-uniform temperature district heating system with decentralized heat pumps and standalone storage tanks. *Energy, 170*, 931–941. https://doi.org/10.1016/j.energy.2018.12.209

Arabkoohsar, Ahmad, Behzadi, A., & Nord, N. (2021). A highly innovative yet cost-effective multi-generation energy system for net-zero energy buildings. *Energy Conversion and Management, 237*, Article 114120. https://doi.org/10.1016/j.enconman.2021.114120

Barbieri, E. S., Dai, Y. J., Morini, M., Pinelli, M., Spina, P. R., Sun, P., & Wang, R. Z. (2014). Optimal sizing of a multi-source energy plant for power heat and cooling generation. *Applied Thermal Engineering, 71*(2), 736–750. https://doi.org/10.1016/j.applthermaleng.2013.11.022

Behzadi, A., & Arabkoohsar, A. (2020). Comparative performance assessment of a novel cogeneration solar-driven building energy system integrating with various district heating designs. *Energy Conversion and Management, 220*, Article 113101. https://doi.org/10.1016/J.ENCONMAN.2020.113101

Behzadi, A., Arabkoohsar, A., & Perić, V. S. (2021). Innovative hybrid solar-waste designs for cogeneration of heat and power, an effort for achieving maximum efficiency and renewable integration. *Applied Thermal Engineering*, (February), 190. https://doi.org/10.1016/j.applthermaleng.2021.116824

Behzadi, A., Arabkoohsar, A., & Yang, Y. (2020). Optimization and dynamic techno-economic analysis of a novel PVT-based. *Applied Thermal Engineering*. , Article 115926. https://doi.org/10.1016/j.applthermaleng.2020.115926

Behzadi, A., Gholamian, E., Houshfar, E., Ashjaee, M., & Habibollahzade, A. (2018). Thermoeconomic analysis of a hybrid PVT solar system integrated with double effect absorption chiller for cooling /hydrogen production. *Energy Equipment and Systems, 6*(4).

Bet Sarkis, R., & Zare, V. (2018). Proposal and analysis of two novel integrated configurations for hybrid solar-biomass power generation systems: Thermodynamic and economic evaluation. *Energy Conversion and Management, 160*, 411–425. https://doi.org/10.1016/J.ENCONMAN.2018.01.061

Buonomano, A., Calise, F., Palombo, A., & Vicidomini, M. (2017). Adsorption chiller operation by recovering low-temperature heat from building integrated photovoltaic thermal collectors : Modelling and simulation. *Energy Conversion and Management*. https://doi.org/10.1016/j.enconman.2017.05.005

Compton, M., & Rezaie, B. (2018). Investigating steam turbine feasibility to improve the sustainability of a biomass boiler using TRNSYS. *Sustainable Cities and Society, 43*(February), 86–94. https://doi.org/10.1016/j.scs.2018.08.032

Das, B. K., Tushar, M. S. H. K., & Hassan, R. (2021). Techno-economic optimisation of stand-alone hybrid renewable energy systems for concurrently meeting electric and heating demandh. *Sustainable Cities and Society, 68*, Article 102763. https://doi.org/10.1016/j.scs.2021.102763

Duan, X., Xu, Z., Sun, X., Deng, B., & Liu, J. (2021). Effects of injection timing and EGR on combustion and emissions characteristics of the diesel engine fuelled with acetonebutanolethanol/diesel blend fuels. *Energy (Oxford), 231*, 121069. https://doi.org/10.1016/j.energy.2021.121069

Ekanayake, J. B. (2020). Optimal Placement, Sizing and Power Factor of Distributed Generation: A Comprehensive Study Spanning from the Planning Stage to the Operation Stage. *Energy*. https://doi.org/10.1016/j.energy.2020.117011

Ferreira, A. C., Nunes, M. L., & Teixeira, S. F. C. F. (2020). *Thermodynamic and economic optimization of a solar-powered Stirling engine for micro-cogeneration purposes, 111*(2016), 1–17. https://doi.org/10.1016/j.energy.2016.05.091

Franco, A., & Fantozzi, F. (2016). Experimental analysis of a self consumption strategy for residential building : The integration of PV system and geothermal heat pump. *Renewable Energy, 86*, 1075–1085. https://doi.org/10.1016/j.renene.2015.09.030

Gholamian, E., Ahmadi, P., Hanafizadeh, P., & Ashjaee, M. (2020). Dynamic feasibility assessment and 3E analysis of a smart building energy system integrated with hybrid photovoltaic-thermal panels and energy storage. *Sustainable Energy Technologies and Assessments, 42*. https://doi.org/10.1016/j.seta.2020.100835

Gholamian, Ehsan, Hanafizadeh, P., Ahmadi, P., & Mazzarella, L (2020a). 4E analysis and three-objective optimization for selection of the best prime mover in smart energy systems for residential applications: a comparison of four different scenarios. *Journal of Thermal Analysis and Calorimetry*. https://doi.org/10.1007/s10973-020-10177-0

Gholamian, Ehsan, Hanafizadeh, P., Ahmadi, P., & Mazzarella, L (2020b). A transient optimization and techno-economic assessment of a building integrated combined cooling, heating and power system in Tehran. *Energy Conversion and Management, 217*, Article 112962. https://doi.org/10.1016/J.ENCONMAN.2020.112962

Ghorab, M., Canada, N. R., Drive, H., & Ka, O. N. (2019). Energy hubs optimization for smart energy network system to minimize economic and environmental impact at Canadian community. *Applied Thermal Engineering, 151*(December 2018), 214–230. https://doi.org/10.1016/j.applthermaleng.2019.01.107

Habibollahzade, A., Gholamian, E., Ahmadi, P., & Behzadi, A. (2018). Multi-criteria optimization of an integrated energy system with thermoelectric generator, parabolic trough solar collector and electrolysis for hydrogen production. *International Journal of Hydrogen Energy, 43*(31), 14140–14157. https://doi.org/10.1016/J.IJHYDENE.2018.05.143

Harmouch, F. Z., Krami, N., & Hmina, N. (2018). A multiagent based decentralized energy management system for power exchange minimization in microgrid cluster. *Sustainable Cities and Society, 40*, 416–427. https://doi.org/10.1016/j.scs.2018.04.001

Ibrahim, A., Fudholi, A., Sopian, K., Othman, M. Y., & Ruslan, M. H. (2014). Efficiencies and improvement potential of building integrated photovoltaic thermal (BIPVT) system. *Energy Conversion and Management, 77*, 527–534. https://doi.org/10.1016/j.enconman.2013.10.033

Kanyarusoke, K., Gryzagoridis, J., & Oliver, G. (2016). Validation of TRNSYS modelling for a fixed slope photovoltaic panel. *Turkish Journal of Electrical Engineering and Computer Sciences, 24*(6), 4763–4772. https://doi.org/10.3906/elk-1502-38

Karami, N., Moubayed, N., & Outbib, R. (2014). *Energy management for a PEMFC – PV hybrid system, 82*, 154–168. https://doi.org/10.1016/j.enconman.2014.02.070

Khalid, F., Dincer, I., & Rosen, M. A. (2017). Thermoeconomic analysis of a solar-biomass integrated multigeneration system for a community. *Applied Thermal Engineering, 120*(Supplement C), 645–653. https://doi.org/10.1016/j.applthermaleng.2017.03.040

Kim, M., Kim, D., Heo, J., & Lee, D. (2019). Techno-economic analysis of hybrid renewable energy system with solar district heating for net zero energy community. *Energy, 187*, Article 115916. https://doi.org/10.1016/j.energy.2019.115916

Klein, S. A. (1988). *TRNSYS-A transient system simulation program*. University of Wisconsin-Madison, Engineering Experiment Station Report, 38–12.

Li, Z. X., Ehyaei, M. A., Kamran Kasmaei, H., Ahmadi, A., & Costa, V. (2019). Thermodynamic modeling of a novel solar powered quad generation system to meet electrical and thermal loads of residential building and syngas production. *Energy Conversion and Management, 199*, Article 111982. https://doi.org/10.1016/J.ENCONMAN.2019.111982

Lin, H., Yang, C., & Xu, X. (2020). A new optimization model of CCHP system based on genetic algorithm. *Sustainable Cities and Society, 52*, Article 101811. https://doi.org/10.1016/j.scs.2019.101811

Luo, X., Zhu, Y., Liu, J., & Liu, Y. (2018). Design and analysis of a combined desalination and standalone CCHP (combined cooling heating and power) system integrating solar energy based on a bi-level optimization model. *Sustainable Cities and Society, 43*, 166–175. https://doi.org/10.1016/j.scs.2018.08.023

Mateo, C., Frías, P., & Tapia-ahumada, K. (2019). A comprehensive techno-economic assessment of the impact of natural gas-fueled distributed generation in European electricity distribution networks. *Energy, xxxx*, Article 116523. https://doi.org/10.1016/j.energy.2019.116523

Nami, H., Arabkoohsar, A., & Anvari-Moghaddam, A. (2019). Thermodynamic and sustainability analysis of a municipal waste-driven combined cooling, heating and power (CCHP) plant. *Energy Conversion and Management, 201*, Article 112158. https://doi.org/10.1016/J.ENCONMAN.2019.112158

Pesaran, H. A. M., Nazari-heris, M., Mohammadi-ivatloo, B., & Seyedi, H. (2020). A hybrid genetic particle swarm optimization for distributed generation allocation in power distribution networks. *Energy.* , Article 118218. https://doi.org/10.1016/j.energy.2020.118218

Rehman, H., Hirvonen, J., Kosonen, R., & Sirén, K. (2019). Computational comparison of a novel decentralized photovoltaic district heating system against three optimized solar district systems. *Energy Conversion and Management, 191*(April), 39–54. https://doi.org/10.1016/j.enconman.2019.04.017

Ren, F., Wang, J., Zhu, S., & Chen, Y. (2019). Multi-objective optimization of combined cooling, heating and power system integrated with solar and geothermal energies. *Energy Conversion and Management, 197*(August), Article 111866. https://doi.org/10.1016/j.enconman.2019.111866

Roselli, C., & Sasso, M. (2016). Integration between electric vehicle charging and PV system to increase self-consumption of an office application. *Energy Conversion and Management, 130*, 130–140. https://doi.org/10.1016/j.enconman.2016.10.040

Sadi, M., & Arabkoohsar, A. (2019). Modelling and analysis of a hybrid solar concentrating-waste incineration power plant. *Journal of Cleaner Production, 216*, 570–584. https://doi.org/10.1016/j.jclepro.2018.12.055

Safaei, A., Freire, F., & Henggeler, C. (2015). A life cycle multi-objective economic and environmental assessment of distributed generation in buildings. *Energy Conversion and Management, 97*, 420–427. https://doi.org/10.1016/j.enconman.2015.03.048

Singh, A. K., & Parida, S. K. (2017). A review on distributed generation allocation and planning in deregulated electricity market. *Renewable and Sustainable Energy Reviews*. https://doi.org/10.1016/j.rser.2017.10.060. *August 2016*, 0–1.

Soloha, R., Pakere, I., & Blumberga, D. (2017). Solar Energy Use in district heating systems. A case study in Latvia. *Energy*. https://doi.org/10.1016/j.energy.2017.04.151

Song, X., Ye, C., Li, H., Wang, X., & Ma, W. (2017). Field study on energy economic assessment of office buildings envelope retrofitting in southern China. *Sustainable Cities and Society, 28*, 154–161. https://doi.org/10.1016/j.scs.2016.08.029

Sun, L., Jin, Y., Pan, L., Shen, J., & Lee, K. Y. (2019). Efficiency analysis and control of a grid-connected PEM fuel cell in distributed generation. *Energy Conversion and Management, 195*(April), 587–596. https://doi.org/10.1016/j.enconman.2019.04.041

Suwanmanee, U., Saebea, D., Hacker, V., & Assabumrungrat, S. (2018). Conceptual design and life cycle assessment of decentralized power generation by HT-PEMFC system with sorption enhanced water gas shift loop. *Energy Conversion and Management, 171*(April), 20–30. https://doi.org/10.1016/j.enconman.2018.05.068

Tong, X., Zhang, F., Ji, B., Sheng, M., & Tang, Y. (2016). Carbon-Coated Porous Aluminum Foil Anode for High-Rate, Long-Term Cycling Stability, and High Energy Density Dual-Ion Batteries. *Advanced materials (Weinheim), 28*(45), 9979–9985. https://doi.org/10.1002/adma.201603735

Torchio, M. F. (2015). Comparison of district heating CHP and distributed generation CHP with energy, environmental and economic criteria for Northern Italy. *ENERGY CONVERSION AND MANAGEMENT, 92*, 114–128. https://doi.org/10.1016/j.enconman.2014.12.052

Vera, D., & Jurado, F. (2018). *Biomass gasi fi cation coupled to an EFGT-ORC combined system to maximize the electrical energy generation : A case applied to the olive oil industry, 144*. https://doi.org/10.1016/j.energy.2017.11.152

Wang, M., Jiang, C., Zhang, S., Song, X., Tang, Y., & Cheng, H. (2018). Reversible calcium alloying enables a practical room-temperature rechargeable calcium-ion battery with a high discharge voltage. *Nature chemistry, 10*(6), 667–672. https://doi.org/10.1038/s41557-018-0045-4

Wang, J., Li, S., Zhang, G., & Yang, Y. (2019). Performance investigation of a solar-assisted hybrid combined cooling, heating and power system based on energy, exergy, exergo-economic and exergo-environmental analyses. *Energy Conversion and Management, 196*, 227–241. https://doi.org/10.1016/J.ENCONMAN.2019.05.108

Wang, J., Lu, Y., Yang, Y., & Mao, T. (2016). Thermodynamic performance analysis and optimization of a solar-assisted combined cooling, heating and power system. *Energy, 115*, 49–59. https://doi.org/10.1016/j.energy.2016.08.102

Wang, B., Ma, F., Ge, L., Ma, H., Wang, H., & Mohamed, M. A. (2021). Icing-EdgeNet: A Pruning Lightweight Edge Intelligent Method of Discriminative Driving Channel for Ice Thickness of Transmission Lines. *IEEE transactions on instrumentation and measurement, 70*, 1–12. https://doi.org/10.1109/TIM.2020.3018831

Xiang, G., Zhang, Y., Gao, X., Li, H., & Huang, X. (2021). Oblique detonation waves induced by two symmetrical wedges in hydrogen-air mixtures. *Fuel*, 295. https://doi.org/10.1016/j.fuel.2021.120615

Xu, X., Niu, D., Xiao, B., Guo, X., Zhang, L., & Wang, K. (2020). Policy analysis for grid parity of wind power generation in China. *Energy policy, 138*, Article 111225. https://doi.org/10.1016/j.enpol.2019.111225

Xu, Y., Yan, C., Liu, H., Wang, J., Yang, Z., & Jiang, Y. (2020). Smart energy systems: A critical review on design and operation optimization. *Sustainable Cities and Society. Vol. 62*. Elsevier Ltd, Article 102369. https://doi.org/10.1016/j.scs.2020.102369

Yan, J., Broesicke, O. A., Wang, D., Li, D., & Crittenden, J. C. (2020). Parametric life cycle assessment for distributed combined cooling, heating and power integrated with solar energy and energy storage. *Journal of Cleaner Production, 250*, Article 119483. https://doi.org/10.1016/J.JCLEPRO.2019.119483

Yang, C., Wang, X., Huang, M., Ding, S., & Ma, X. (2017). Design and simulation of gas turbine-based CCHP combined with solar and compressed air energy storage in a hotel building. *Energy and Buildings, 153*, 412–420. https://doi.org/10.1016/J.ENBUILD.2017.08.035

Yang, G., & Zhai, X. Q. (2019). Optimal design and performance analysis of solar hybrid CCHP system considering influence of building type and climate condition. *Energy, 174*, 647–663. https://doi.org/10.1016/j.energy.2019.03.001

Zhang, X., Tang, Y., Zhang, F., & Lee, C. (2016). A Novel Aluminum-Graphite Dual-Ion Battery. *Advanced energy materials, 6*(11), Article 1502588. https://doi.org/10.1002/aenm.201502588

Zhang, Liang, Wang, Xuesong, Zhang, Zhe, Cui, Ying, Ling, Lyu, & Cai, G. (2021). An Adaptative Control Strategy for Interfacing Converter of Hybrid Microgrid Based on Improved Virtual Synchronous Generator. *IET Renewable Power Generation*. https://doi.org/10.1049/rpg2.12293

Zhu, D., Wang, B., Ma, H., & Wang, H. (2020). Evaluating the vulnerability of integrated electricity-heat-gas systems based on the high-dimensional random matrix theory. *CSEE Journal of Power and Energy Systems, 6*(4), 878–889. https://doi.org/10.17775/CSEEJPES.2019.00440

Zubi, G., Pasaoglu, G., & Dufo-lo, R. (2020). *Photovoltaic thermal hybrid solar collector and district heating configurations for a Central European multi-family house, 148*(2017), 915–924. https://doi.org/10.1016/j.enconman.2017.05.065